Dual Mode Localization Assisted Beamforming for mmWave V2V Communication

Chinmay Mahabal, Honggang Wang, Hua Fang

University of Massachusetts Dartmouth
{cmahabal, hwang1, hfang2}@umassd.edu

***Abstract*—This study is motivated by the fact that localization in Vehicle-to-Vehicle communication becomes a more critical problem because both the terminals of the communication link are in motion. The positional awareness merely based on GPS or local sensors has an error margin of around 10 meters, which can worsen in uncertain real-time conditions such as road topology and highway traffic. The paper analyses the relation between beamforming and beam alignment for highly directive antennas. This is more challenging in the events of localization of transceivers. When the subsystem models presented in this paper are taken into consideration, the joint vehicle dynamics-beamforming approach will improve the SNR for a constant power gain. The vehicle dynamics model is designed to be more realistic considering the non-linear acceleration based on the throttle-brake jerks due to internal engine noises as well as external traffic conditions. The prediction subsystem highlights the flaws of the Kalman Filter for non-linear parameters and the need for an Unscented Kalman Filter. The beamforming strategies are supported by the requirements of localization and the hardware constraints on the antenna due to phase shifters and the number of elements to yield more realistic results.**

***Index Terms*—Beam tracking, beamforming, Vehicle Dynamics, Highway, Unscented Kalman Filter,SNR, Antenna Phassed Array**

I. Introduction

V2V communication is necessary for 5G side-link, resource allocation and traffic management. Vehicular networking is an important cornerstone for Intelligent Transportation Systems (ITS) in the sense that it supports several traffic applications; such as traffic management and safety.These networks require the continuous exchange of status information about the status of the vehicle; such as its position, speed, acceleration, and heading [1].

Vehicular communication can be classified based on the receiving nodes such Vehicle-to-Infrastructure for Roadside Units, Vehicle-to-Network for Base stations or cloud and Direct Vehicle-to-Vehicle(V2V) based on the number of factors like specifications given by the IEEE 802.11p standard, resource allocation, and vehicle density. The proposed work considers the effect of vehicle dynamics and beamforming on direct V2V communication for a highway environment. Literature survey has proved that direct communications using either a dedicated channel or underlay communication using a side-link can reduce the latency for better information sharing. The applications of such V2V can be seen in the events of Connected Autonomous vehicles, Vehicle Platooning, and as a subsystem of Vehicular Networks. In [2] and [3] Cooperative Adaptive Cruise Control uses onboard sensors and communication with surrounding vehicles for homogeneous and heterogeneous vehicles platoons for autonomous vehicles. The awareness of surrounding and information exchange increases the safety and driving experience. It also gives the relation between vehicle traffic density and average vehicle velocity. In such highly interdisciplinary applications, the communication link has to consider Vehicle Dynamics and localization, which continuously changes instantaneous positions and beam coverage zones.

Isotropic antennas for omnidirectional communication use more energy, with low SNR hence beamforming is preferred. Clearly beamforming has important benefits over transmitting with an isotropic antenna, but also has important weaknesses that need to be addressed [1]. Research has been done on Point to Multi-point V2V communication using beamforming which has made possible due to adaptive beamforming. The proposed work will address the optimization problem of adaptive beamforming using localization for the transmitter and receiver. This common scenario makes V2V communication a lot more challenging since it needs to consider dual mode localization. The issue of dynamic transreceivers and obstacle was approached by Markov chain in [4]. These techniques have a spectrum of constraints such frontend- design of antennas and back end- design of precoding matrix which have a joint effect on the efficiency of the V2V system. The proposed paper will design a beamforming technique by considering a frontend model based on third order vehicle dynamic models. These higher order modelling consider non linear accelerations which are close enough to realistic conditions. The relation between external factors and channel frontend model will make the system scale-able and more realistic.

Similar to the work done in [4] and [5], the proposed work assumes an established communication link between the trans-receiver vehicles at time t_0. In V2V communication, beam tracking is challenging due to localization at the both ends(both the vehicles) of the communication link. The positional awareness using V2V leads to overhead communication and beam alignment techniques. The probability of link dropage further increases with more narrower beams. The proposed paper models the vehicle dynamics uncertainties to put constraints on beam width ψ to maximize SNR based on error in position awareness. In our work in our ongoing work

[6], the V2V communication and its effects were seen for a vehicle platoon. However, the proposed work dives deep into a specific issue of connectivity for a case of two vehicles which can be scaled to point-to-multipoint applications.

Contributions of our paper:

1) Modelling dual mode third order vehicle dynamics and thus establish relation between vehicle dynamics and beam alignment. Most of the current literature assumes on order 1 in vehicle dynamics while analysing beamforming. The constant velocity, thus affecting the vehicle localization's pos_a and pos_b with time. The proposed work considers the variation of acceleration and jerk along with velocity and position. The beam alignment error θ_e and beam switching speed are affected by such higher orders and thus necessary to study the vehicle dynamics while designing V2V communication.
2) The paper simulates the effect of Antenna design on optimization problem of SNR, beam alignment θ and beam forming angle ψ. These results are act to fill in the research gap between the relation of vehicle dynamics and the hardware constraints of antenna elements and phase shifters. Building on the hardware design, the work surveys the existing methods and challenges in narrow beamforming to simulate the errors in beam alignment and Directivity.
3) Parameter Estimation: The beam alignment error θ_e is not only affected by third order vehicle dynamics but by communication channel losses, domino effect of surrounding traffic and road topologies and vehicle power train delay. The proposed work considers the threshold for these losses while deciding the error margin
4) For a narrow beamwidth ψ, the coverage area changes with the change in pos_a and pos_b and the resultant d_{ab} distance between them. Thus adaptive beamforming and beam steering are important for V2V with third order.The main goal beamwidth threshold ψ_{th} is to keep the vehicle in coverage area, thus it should consider the dynamic θ_e margins. This makes ψ dynamic too.
5) Finally, the work analyses the effect on channel communication quality QoS due to above measures of beamforming for a V2V scenario. The link quality deteriorates as a function of the lane width and relative positions of the vehicles. The mathematical models and simulations for the SNR and and link probability are presented.

The paper is organized in the similar flow where section II mentions the relevant literature, section III elaborates on the system model. These subsystems are explained in the later sections where section IV classifies different Vehicle Dynamics, Section V on its effects on Beam Alignment. The prediction methodology using Kalman Filter and later the Unscented Kalman Filter has been implemented in Section VI.Section VII and VIII explain the Beamforming and Beam steering from hardware constraints point of view. All the challenges and its consequent effects on link quality are explained in the section IX of Channel Quality of Service.

II. Literature Review

TABLE I: Survey of Environment conditions for V2V

Vehicle Dynamics (VD)	Independent	Single Mode (V2I)	Dual Mode (V2V)
Assumed	[7]		[8] [1]
Velocity	[9]		[10]
Acceleration	[11] [3]	[12] [13]	[2]
Jerk	[2] [14]	[15]	Our Paper

The first column for Independent mode focusses on the vehicle dynamics and its effect on Antenna beamforming. However their focus is not mostly on the type of localization. In Vehicle- Basestation communication or Vehicle-RSU communication only one node is in motion and classified as Single mode communication. There has been considerable research work in beam alignment for V2V communication, assisted by position prediction techniques, but they have assumed the vehicle dynamics, which can be classified in first row. The last column classifies the dual mode localization in V2V communication and its effect on beam alignment. A similar classification was seen in [16] where The authors classified the geometry model as Fix to mobile (F2M), M2M, and Air to Ground (A2G) to study effect of mobility on wireless communication. The geometry can be classified as Stochastic and Deterministic model with the transmission model as 2D or 3D based on the applications. Most of the events in the proposed scenario assumes two vehicles in parallel lanes with different vehicle dynamics. Velocity of vehicle A is higher hence it will overtake vehicle B over period t, which will lead to variable beam alignment angle θ and beamwidth ψ as seen in Fig. 3. The other trajectories include along a curved path, merges and lane exits. [12] uses communication with RSU for a vehicle along straight and curved trajectory. The curved trajectory makes it vital to consider the position as a 2D coordinate system. However, in the given proposal since the vehicles are assumed along parallel straight highways, single axis movement is gives enough information.

In [2] Cooperative Adaptive Cruise Control uses onboard sensors and communication with surrounding vehicles to maintain safe headway space distance. This performance decides the string stability in homogeneous and heterogeneous vehicles platoons for autonomous vehicles. [3] analyses the butterfly effect of shockaves due to acceleration or breaks in dense traffic scenarios. It also gives the relation between vehicle traffic density and average vehicle velocity. In [12], the vehicle position prediction is implemented without system model, however, it assumes a constant acceleration by stating $\alpha_{t-1} \approx \alpha_t \approx \alpha_{t+1}$.

Work on adaptive beamforming for P2MP has been done in [17] to show that Delivery ratio is affected by beamwidth varying between 5 to 30 $\circ$ and vehicle density from 60 to 160 vehicles/km. It states the error in GPS is high. [17] [18]. [19] has classified the errors in GPS localization which include Geometric dilution, Emphemeris errors, Satellite clock errors, Atmospheric errors and multipath effects.

To compensate for such losses, the proposed work uses Unscented Kalman Filter in parameter estimation. [16] Compares 4 channel estimation algorithms based on their Prior Information, Complexity, Performance. Amongst Linear Square(LS), Minimum Mean Square Error(MMSE, Wiener Filter), Recursive Least Square and Kalman Filter, the last one has good performance for dynamic state space models and provide accurate tracking. [12] uses MUSIC algorithm without any state model. However the V2I communication requires position estimation at the vehicle and RSU during the Angle of Arrival and Angle of Departure calibration. [20] uses Enhanced Kalman Filter for 5G based V2V communication. The research evaluates SNR performance for high mobility environments for channel estimation and to improve estimation accuracy. The SNR gain increases by 7.5 dB for high speed environments. [21] uses adaptive beam tracking to improve the SNR using Unscented Kalman Filter. The state estimation error in this paper was reduced using constrained suboptimal beams and sounding beamformers. The SNR is calculated as a function of tracked CSI with the gain for prediction between $\pm$ 1 dB. The state prediction can improve SNR when the losses increase.

The literature survey establishes a comparison between two main pillars of V2V communication, the vehicle dynamics shown as rows and the communication modes shown as columns. For an effective V2V communication model, it is imperative to have realistic vehicle dynamic model upto third degree which considers the non linear acceleration.The columns highlight the difference between communication modes where in V2I we have stationary base station and hence a single mode localization where as V2V has a dual mode localization. Few of the researchers have assumed the perfect communication link while elaborating the vehicle movement dynamics. The proposed research paper will address this research gap.

III. System Model

The Vehicle Dynamics(VD) block generates the positions of the target vehicles. Based on the control input and noise characteristics, the dynamics can be classified as first, second and third order, which have been elaborated in the later section. The sensor fusion [22] is responsible to monitor the parameters $[J, \alpha, v, pos]$ of VD and decides which values need to be sent to the communication channel based on the vehicle dynamics and the protocol requirements. Increase in the parameters will improve the accuracy at the cost of throughput and communication overload. The instantaneous position is the primary parameter sent to the Beam Alignment subsystem. A similar dual mode communication has been used in [23] for platoon safety where sensory and communication data was exchanged between the leader and follower vehicles. The accuracy of this location directly affects the beam tracking and thus the link probability of communication channel. When the vehicles use beamforming instead of isotropic antenna, the uncertainties in vehicle dynamics can result in NLOS communication events, leading to sudden drop in SNR values. The retransmissions of packets in such cases leads to increased latency.

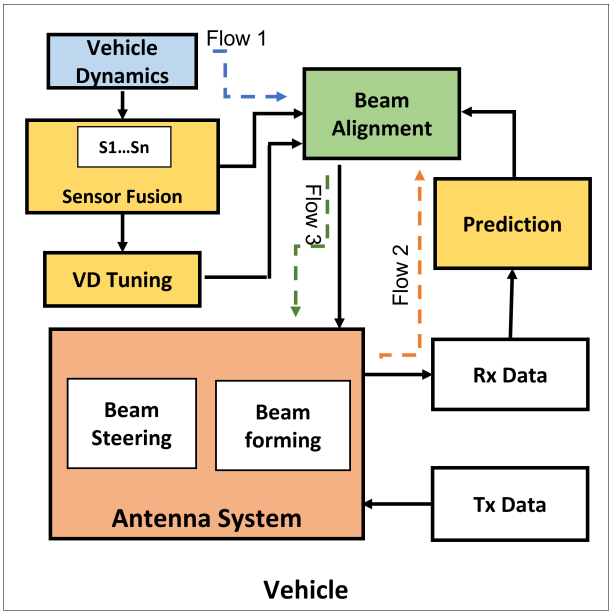

Fig. 1: System Diagram

The VD Tuning sends the initial conditions of velocity and acceleration and boundary limits of the parameters which need to be used by Prediction subsystem and Beam alignment. This also includes the prediction noise and measurement noise co variances used by the KF or UKF systems.

The data received from the Antenna System is corrupted with noise due to external factors such traffic and road topologies, internal factors such engine and powertrain losses and channel characteristics. To get more reliable data, the Prediction subsystem is used for signal processing before the VD of the corresponding car are sent for Beam Alignment. A similar Prediction Filter can be used for sensor fusion of the ego vehicle as well, however, since there is no wireless communication over a long range distance, we have assumed negligible sensor noise so we can skip the Prediction block from Flow 1 and mainly use it during Flow 2. For V2I communication, one of the node (Base station or RSU) is stationary [13] which makes beam alignment an independent block however for the proposed V2V communication, the beam alignment performance is affected by both the vehicle dynamics and errors in positional awareness of the ego and target vehicle.

As explained in later section, the beam alignment is based on relative positions of ego vehicle and transmitter vehicle 'A' which can be seen in the synchronous Data Flow 1 and Data Flow 2. A certain time lag in the Flow 2 will thus affect the beam alignment accuracy. This lag can be considered as a part of communication noise while processing the signal at Prediction block.

Once the beam alignment angle θ is estimated, this along with positional errorpos_e and is sent to the Antenna System to calculate relative distance error d_e as a part of Data Flow 3. This system tries to align the θ as close to the actual radial

angle between the vehicle θ_v. The error, based on the alignment sensitivity $\Delta\theta$ and d_e is compensated with beamforming angle ψ. The hardware and vehicle dynamics dependency of the Antenna System is explained in later sections.

IV. Vehicle Dynamics

TABLE II: Vehicle Dynamics Orders

Order	Jerk (J)	Acc (α)	Vel (v)
First	0	0	k_v
Second	0	k_a	$\int_0^t \alpha\, dt$
Third Linear	J	$\int_0^t J\, dt$	$\int_0^t \alpha(t)\, dt$
Third Non Linear(NL)	$J(t)$	$\int_0^t J(t)\, dt$	$\int_0^t \alpha(t)\, dt$

The table II gives the equations for the three Vehicle Dynamics (VD) parameters. The position can be calculated by Eq. 1 which is similar for all the orders. The complexity of the final position vector increases as we go down the order. The mathematical representation of the above table can be given as follows.

$$\begin{bmatrix} pos_{t+1} \\ v_{t+1} \\ \alpha_{t+1} \end{bmatrix} = \begin{bmatrix} 1 & T & 0 \\ 0 & 1 & T \\ 0 & 0 & T + J/\alpha_t \end{bmatrix} \begin{bmatrix} pos_t \\ v_t \\ \alpha_t \end{bmatrix} \quad (1)$$

Where $v = \dot{pos}$, $\alpha = \dot{v}$ and $J = \dot{\alpha}$.

A. Localization for a single vehicle

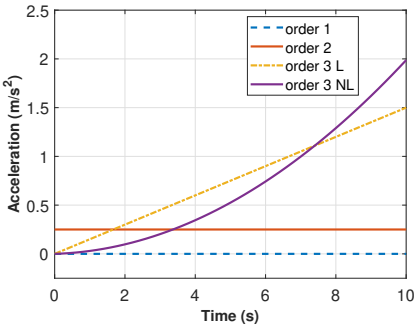

Fig. 2: Orders in Vehicle Dynamics

The Fig. 2 shows the variation of acceleration α of the vehicle while considering different orders of the vehicle dynamics by substituting $\alpha = 0.25m/s^2$, $J = 0.03m/s^3$, $J(t) = [J_{0to45}, J_{45to55}, J_{55to150} = [00.5 - 0.5]$ in the table II and Eq. 1. As seen in Table I,most of the research in beam alignment consider the basic first order kinematic equations with the acceleration is 0. In such conditions the vehicle moves with constant velocity . For second order equations, the vehicle moves with a constant acceleration. In real time the engine throttle brake conditions are non linear in nature. Hence the acceleration rarely follows a constant trajectory. In the so-called third order vehicle dynamics, the equations have non-zero jerks. For a constant value of jerk, we see a linear acceleration [14] [24]. The extreme throttles are followed by a brake to maintain the vehicle velocity within the traffic regulation bounds and safety reasons. Reasons of non linear acceleration can also be road topologies, variation in vehicle traffic or internal factors such as engine performance and disturbances due to manual driving.

We assume that the state of each vehicle remains unchanged during a single transmission epoch with a duration of $T = \Delta t$. In the above figure 2 randomly induced jerk(change in acceleration) are placed within the peaks of $\pm 5m/s^3$ based on the works of [14] where the driving styles of an expert and average drivers were compared. Ideally for a smooth driving experience, the jerks should be 0. These alternating peaks also impose constraints on the acceleration and velocity value to maintain realistic values.

B. Dual Mode Localization

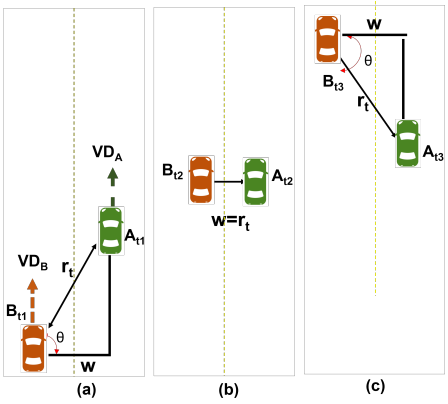

Fig. 3: Alignment angle θ_v during an overtake event. (a) Vehicle B approaches A.(b) Vehicle B and A are in parallel lanes adjacent to each other. (c) Vehicle B has overtaken A.

In the previous section we have seen how the VD order determines the VD parameters for a given vehicle. As seen from the system model 1, θ is dependent on relative positions of the vehicles, hence it is necessary to consider Dual Mode Localization (DML) where the transmitter and receiver are in motion. This scenario distinguishes V2V from V2I communication. The figure 3 shows positions of vehicles A and B at three time instants. For the trajectories of these vehicles along the parallel lanes, the lateral deviation is assumed to be zero making road width w a constant.

$$v_B \geq v_A \quad (2)$$

$$pos_{A,t} = pos_{B,t} - t(v_A - v_B) \quad (3)$$

where pos_A,pos_B,v_A and v_B are the positions and velocities of the vehicles moving in same direction along two parallel lanes as shown in figure 7. The above Eq. 3 make it obvious that over a time, vehicle B overtakes vehicle A. When the vehicles are moving in the opposite directions, the V2V contact time is too short to establish the communication link hence currently out of scope of this research.

$$\theta(t) = tan^-1(\frac{pos_{A,t} - pos_{B,t}}{w}) \quad (4)$$

The above equation can verified using the Fig. 3 where w is the width of lane.

V. Vehicle Dynamics for Beam Alignment

A. Relation between VD , θ and ψ

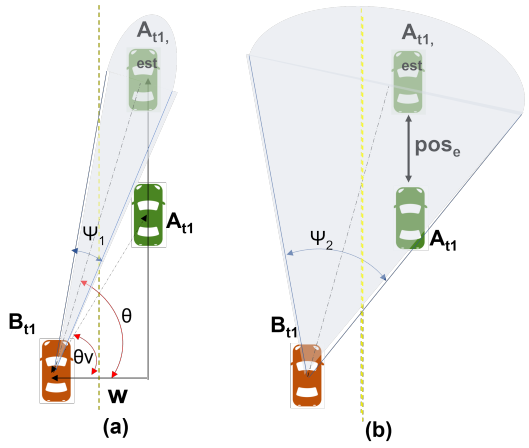

Fig. 4: Coverage probability for constant θ_e and variable beamwidth psi

The figure 4a shows a common scenario on highway where two vehicles in parallel lanes moving with velocity 20 m/s and 15 m/s. For a sufficiently narrow beamwidth ψ, the pos_a may go beyond the beam coverage with a change in VD parameters $[J, \alpha, vel, pos]$. This loss in communication link needs to compensated with a perfect beam alignment angle θ equal to vehicle alignment angle between A and B, θ_v.

The figure 4b shows the effect of change in vehicle dynamics of vehicle B. The error in beam alignment is given by $\theta_e = \theta_v - \theta$. θ_e is a function of prediction accuracy of VD parameters, mainly positional error,pos_e and are significant in DMLs. This positional error affects the relative distance between the vehicles and also referred as d_e in later sections, where $d_e = pos_{A,est} - pos_{B,est}$

The effect of d_e can be reduced by increasing ψ as shown in Fig. 4b. Larger ψ leads to increased energy consumption. The Fig. 4 also shows a relation between ψ and θ_e

The beam steering by angle θ can be implemented by either mechanical rotation or electronically changing the beamforming antenna weights [25]. The later is preferred due to less energy consumption. However, the beam switching is limited by the transmission delay, beamwidth, RF chain activation and the relative velocity between the two vehicles.

In the Fig. 5 the relation between beam steering and beamforming angle is shown for a V2V. The actual alignment angle between θ_v is traced by the beam alignment angle θ.This figure also establishes a relation between beamwidth ψ and beam alignment angle θ. For an omnidirectional antenna on vehicle B(ego vehicle) with infinite range, Beamwidth threshold $\psi_t = +180$ to -180, the probability of vehicle A being in the coverage area is 1. However for a certain beamwidth ψ, it is not required to adjust θ for every time instant. This constrain is given by the equation

$$\psi \leq \Delta\theta = \theta_{t+1} - \theta_t \tag{5}$$

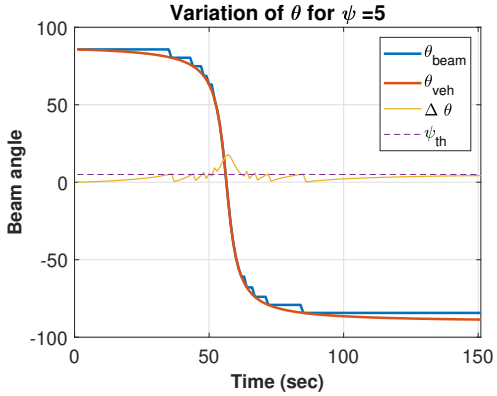

Fig. 5: Beam tracking for second order

This loss in communication can be seen when the $\Delta\theta$ crosses the ψ_t. This $\Delta\theta$ is difference between two beam alignment angles, $\Delta\theta = \theta_{t+1} - \theta_t$. As θ is tangent function seen in Eq. 4, there is a sudden rise along 0 ∘ where vehicle B overtakes A where the communication link is 0. However, wider ψ has lower power efficiency and smaller ψ leads to loss of communication link.

In the Fig. 5 the effect of constant acceleration and non linearity in the position(wrt Fig. 8b) can be seen as the $\Delta\theta$ crosses the ψ threshold upto 17 ° for a period of 10 secs from t_{50} to t_{61}. During this period the two vehicles are out of the communication link and rely on the secondary side lobes which hampers the QoS. As the vehicle B approaches the leader vehicle A (t_0 to $t_7$5), θ_{veh} changes non-linearly since it is proportional to the tangent of the distance between them. Thus the value of $\Delta\theta$ is not constant for every time instant and increases during the event of overtake. When $\Delta\theta$ increases above the ψ threshold, the vehicle communication link disrupts as vehicle A is outside the coverage area of vehicle B.

Secondly, a smaller ψ leads to frequent changes in beam steering which can be seen in Fig. 5 and Fig. 19. A small ψ gives higher accuracy but at the cost of communication overload due to frequent steps and loss of QoS, especially during overtake events.

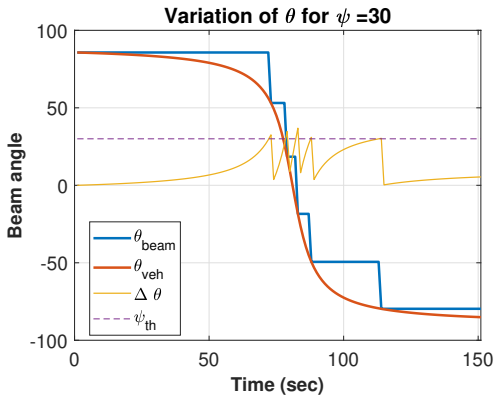

Fig. 6: Beam tracking for wider ψ

Smaller ψ increases the SNR but the system complexity increases as the beam switching instances (seen as steps in θ_{beam}). As seen in figure 19, as the ψ increases, the number of switching instances have been reduced to 5 from 25 (blue steps) in Fig. 5. The beam alignment complexity further increases with higher order vehicle dynamics and adaptive beamforming.

B. Vehicle Alignment Angle

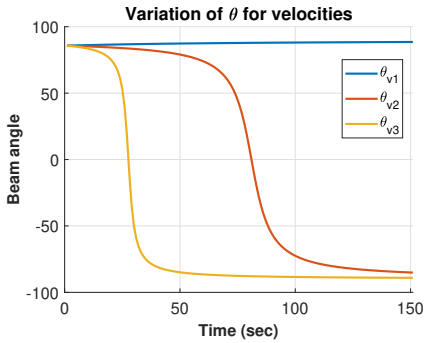

Fig. 7: Variation θ for v_A = 15 m/s and v_{B1},v_{B2},v_{B3} as 10,15,30 m/s

The Fig. 7 shows the relation between v and θ_v. This change in velocity can be inferred from the change in slope of θ_v where steeper slope(orange) corresponds to higher velocity. The value of $\theta_v = 90$ corresponds to Fig. 3a, as the vehicle B approaches vehicle A, the θ_v and effectively θ decreases from 90 to 0 °. $\theta_v = 0$ is for 3b where the vehicle B is about to overtake A. When the vehicle B, overtakes A, θ changes from positive to negative. Further, the angle approaches -90 as the distance between the vehicles increase. In [26], a similar Beam-tracking algorithm is developed to support the mobile transmission up to 100Km/hr in the 120-degree of sector angle.

The four vehicle dynamics levels explained in Fig. 2 and Table 3 are used as foundation to calculate the instantaneous positions of Vehicles A and B. Eq. 1 is then used to calculate the alignment angle. The following graphs elaborate how the slope increases with the VD levels thus affecting the θ and communication QoS.

C. First and Second order VD

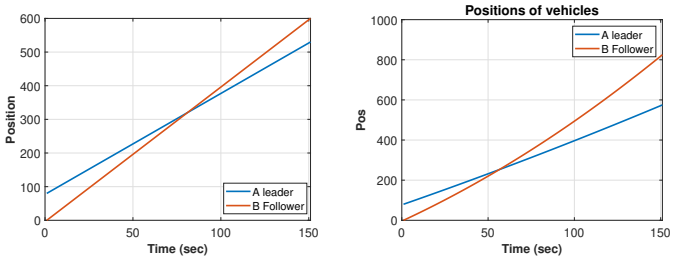

Fig. 8: Position of vehicles for First and Second order

In the figure 8, a first and second order vehicle dynamic for two vehicles is shown. There is enough literature for first order Beam Alignment and can be easily plotted by referring Table II and Eq. 1- [4]. The paper is focused on the effects of higher orders VD beam alignment. For figure 8 a,with constant velocities, the follower vehicle has a higher velocity than the leader, hence obviously it overtakes the leader vehicle around time t=75 secs. This event can be seen where the position graphs intersect and later the distance covered vehicle B increases.

D. Third order VD Beam Alignment

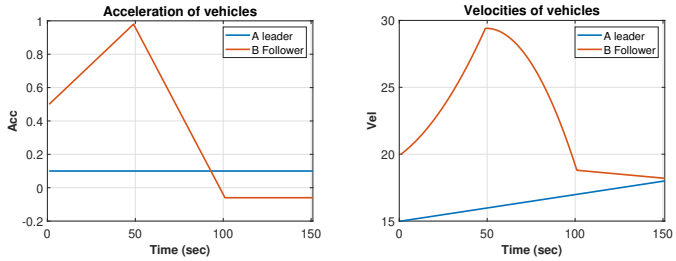

Fig. 9: Acceleration and Velocities of vehicles for Third order

The complexities of higher order have to be considered for both the vehicles in the DML scenario, as shown by the blue and red plots for Vehicle A and B. The third order has non zero Δ_{acc}, which is either constant for linear acceleration or time varying for non-linear as shown in figure 9a. In the given scenario, the acceleration increases to 0.9m/s^2 and then drops to -0.1 m/s^2. This generates a non linear velocity for the vehicle seen in figure 9b.

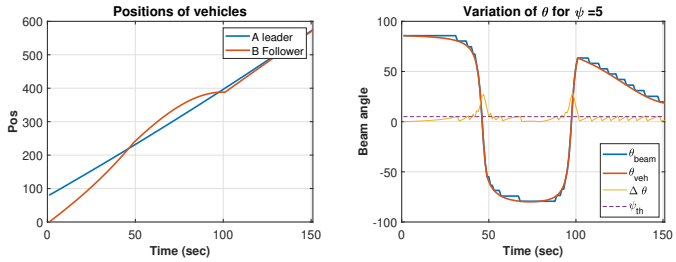

Fig. 10: Position and Beam Alignment for Third order

The Fig. 10 is an extension of previous figure and the VD parameters are generated using Eq. 1. The point where the positions intersect refer to the overtake events. The highly non linear accelerations and deceleration lead to two overtake events as seen in the figure. It can also be noted that the $\Delta\theta$ crosses the ψ_{th} twice, with a higher value as compared to second order to up 25 degrees, leading to greater radio silences. Thus it makes it very crucial to consider these higher order dynamics which are very common in real time vehicular traffic, if a higher accurate beam alignments are to be expected in the V2V communication.

VI. Prediction using Kalman Filter

A. Basic Kalman Filter

Kalman filter proposed by R. E. Kalman in 1960, is an algorithm that uses a series of noisy observed data, which

contains interference and other inaccuracies, to estimates unknown variables with more accuracy.In mathematical terms we would say that a Kalman filter estimates the states of a linear system. The Kalman filter not only works well in practice, but it is theoretically attractive because it can be shown that of all possible filters, it is the one that minimizes the variance of the estimation error. The applications of Kalman filter are found in the fields of target tracking and navigation, such as calculations of spacecraft orbit, tracking of maneuvering target and positioning of GPS [27] [28]. The state estimator of the Kalman filter is used to estimate the state of a dynamic system of real world dynamics. The general assumption in a Kalman filter is that there is some dynamic system which is measured by sensors, and a known control input such as throttle and brake is applied to the dynamic system. In the proposed paper desired estimate is that of position, velocity required to track the vehicle continuously [29].

The work done in [21] uses Unscented Kalman Filter for channel prediction. Here the vehicle moves with known velocity and these sigma variance is 0.1. However, in the proposed result, the sigma is considered to be 10, which is greater and close enough to GPS error as shown in the work of [17]. The designed method has analysed most of the uncertainties and extensive simulation in Matlab. Many physical process such as car trajectory can be approximated as linear process. A linear system is simply a process that can be described by the following two equations: Kalman Filter Estimation has two main stages of Prediction and Measurement and the data is recurssive between these two stages of state model and Covariance matrix calculation respectively. [3] elaborates on the communication delays experienced in VANET using IEEE 802.11p. In this case, elementary laws of physics say that the velocity v and thus state matrix x will be governed by the following equation

Prediction:

Predicted State Estimate:

$$\hat{x}_{k+1} = Ax_k + Bu_k \tag{6}$$

where $A = \begin{bmatrix} 1 & T \\ 0 & 1 \end{bmatrix}, B = \begin{bmatrix} T^2/2 \\ T \end{bmatrix}$

Predicted Process Covariance Estimate based on previous state is given by

$$\hat{P}_{(-)} = AP_{(-)}A' + Q \tag{7}$$

The state vectors will be perturbed by noise due to gusts of wind, potholes, and other unfortunate realities. The noise is a random variable that changes with time [27]. The negative suffix indicates the apriori state and the $\hat{.}$, indicates the estimate value. Q is the process covariance matrix, R is observation error. $Q = \begin{bmatrix} \Delta x_p^2 & \Delta v_p \\ 0 & \Delta v_p^2 \end{bmatrix} R = \begin{bmatrix} \Delta x_R^2 & 0 \\ 0 & \Delta v_R^2 \end{bmatrix}$

Measurement Update:

Calculation of Kalman Gain

$$K = \frac{\hat{P}_{(-)}H'}{H\hat{P}_{(-)}H' + R} \tag{8}$$

and H is the identity matrix. This value of Kalman gain compares the error in state prediction and error in measurement.

Output equation:

$$y_k = H\hat{x}_k + z_K \tag{9}$$

and H is an identity matrix. Update for the posterior covariance process matrix is given by

$$P_{(+)} = (1 - KH)P_{(-)} \tag{10}$$

Update for the State Estimate matrix is given by

$$x_{k+1} = \hat{x}_k + K(y_k - H.\hat{x}_{k+1}) \tag{11}$$

where Y is measured value using the sensors.

In the above equations A, B, and C are matrices; k is the time index; x is called the state of the system; u is a known input such as acceleration to the system; y is the measured output at time t; and w and z are the process noise and measurement noise.X is a state vector of the system and y is the measured value of function of x. [27].

The results show that, the beamforming technique can sustain uncertainties by using Kalman Filter prediction, optimization of beam angle and beam alignment and improvement in SNR.

B. Kalman Filter for various orders of Vehicle Dynamics

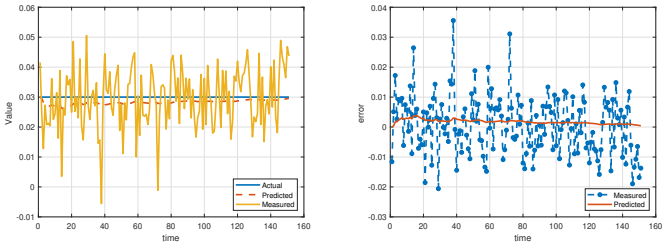

Fig. 11: Kalman Filter for estimation of rate of change of acceleration for the Vehicle

1) Third order Acceleration rate: The vehicle A is moving with linear acceleration cause by constant J=0.3. For an accurate positional awareness, this third ordered data is communicated. The measured covariance matrix R, considers the transmission noise, measurement and power train reaction delay. This noisy measurement can be seen with the values having an error margin of R= ± 0.01. The Kalman filter predictions are more close to the real values with the Prediction noise R= ± 0.001. The figure 11b plots the estimation error with the real values. The Filter successfully predicts with the maximum measurement error of 0.03, ten times higher than than Kalman estimation error of 0.0031 with the error gradually reducing as the time samples increase.

2) Acceleration: We can see the performance of Kalman Filter prediction reducing for a linear rise in the acceleration. This error accumulates as it moves through the vehicle dynamics layers causing an increased positional error. For the given figure 12, R= 0.1 and P is 0.001.

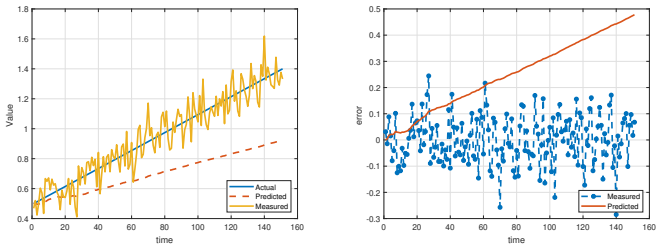

Fig. 12: KF for acceleration estimatinon

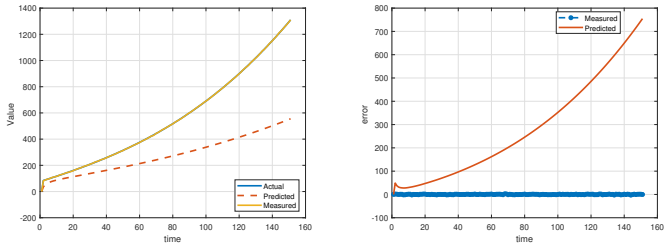

Fig. 13: Position of vehicles for First order

3) First order Position: The figure 13 shows estimation error in Kalman Filter when a third order dynamic movement is subjected to first order communication. As seen, the error exponentially increases and slope limited. Kalman Filter is recursive in nature and uses the previous state estimate which makes it difficult to track linear and exponential values. However, in real time traffic scenarios, vehicles seldom follow a constant velocity trajectory.

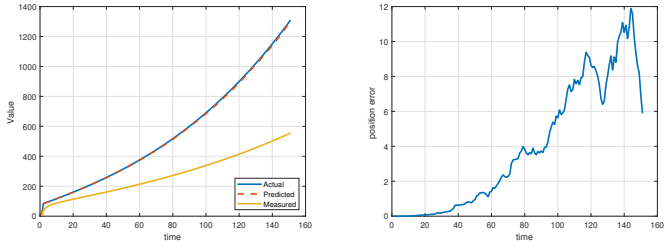

Fig. 14: Position of vehicles for First and Third order

4) Third order Position: In the above figure 14a, the Kalman Filter can successfully predict the exponentially rising position values if the third order acceleration rate is estimated at the initial stage. The figure 14b shows the error between the actual position and estimated position which is less than 12m whereas, for first order communication it rises above 500 m.

The smaller error margins can help maintain a narrow ψ which has been elaborated in the further sections.

C. Unscented Kalman Filter

Based on works of [30], UKF addresses the approximation issues in KF and EKF. As seen in equation 1 and 4 we use the approximate values of state estimate and measurement values for prediction. However these are the Gaussian Random

TABLE III: Performance of KF and UKF

Parameter Sensed	Parameter Predicted	$\Delta_{N,0}$	σ_p, σ_r σ_p, σ_r	error KF/UKF error measured	Fig
Linear α	KF α	0	10^{-3}, 10^{-2}	[0.2, 2.5] 10^{-3}	11
Non linear α	KF α	1	10^{-2}, 0.1	$[160, 5]10^{-3}$	12
pos	KF pos	10^3	1,1	500,1.2	14
α	KF pos	10^3	1,1	10 ,600	13
pos	UKF pos	10^3	1,3	5,12	23

variables propagated through non linear system. This can be specified by use of specifically chosen sample points to capture true mean and covariance and then the posterior mean and covariance.

Measurement Stage: The statistics are calculated using Unscented Transformation. The propagation of random variable x has dimensions L based on number of states. The sigma vectors is formed by matrix χ_i where i is of length 2L+1, and every vector χ_i is assigned a weight W_i [31] [30].

$$\chi_0 = x \tag{12}$$

$$\chi_{1...2L} = x \pm \sqrt{(L+\lambda)P_x} \tag{13}$$

$$W_m = \lambda/(L+\lambda) \tag{14}$$

$$W_c = \lambda/(L+\lambda) + (1-\alpha^2+\beta) \tag{15}$$

$$W_i = Wc = 1/2(L+\lambda) \tag{16}$$

where λ is a scaling factor, given by $\alpha^2(n+k)-n$ where k is between(0a nd $\inf$) and α is between (0,1).

β is secondary scaling parameter, usually set to 2 [32]. The square root $\sqrt{(L+\lambda)P_x}$ is calculated using Choelsky decomposition from lower triangular matrix. These sigma vectors are propagated through non linear functions The measurement vector is given by

$$Y_i = h(\chi_i) i = 0..2L \tag{17}$$

$$y = [\sum_{i=0}^{2L} W_{m,i} Y_i] \tag{18}$$

Correction stage The mean and covariance are approximated using weighted sample mean and covariance of posterior sigma points

$$P_{xy} = [\sum_{i=0}^{2L} W_c (Y_i - x)(Y_i - y)'] \tag{19}$$

$$P_{yy} = [\sum_{i=0}^{2L} W_c (Y_i - y)(Y_i - y)'] \tag{20}$$

Kalman Gain

$$K = \frac{\hat{P}_{xy(-)} H'}{H \hat{P}_{yy(-)} H' + R} \tag{21}$$

The update equations are same as Kalman Filter where update for the posterior Covariance process matrix and State estimate matrix is given by

$$P_{(+)} = (1 - KH) P_{(-)} \tag{22}$$

$$x_{k+1} = \hat{x}_k + K(y - H.\hat{x}_{k+1}) \tag{23}$$

where Y is measured value using the sensors.

D. Simulation and Setup

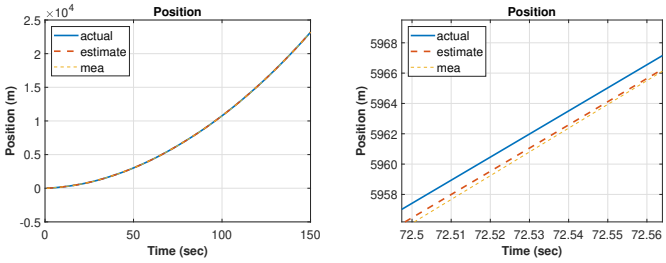

Fig. 15: UKF estimation

The above figures show a third order vehicle dynamic with $J = 0.05$,$\alpha = 2m/s^2$, $v = 15m/s$ and with prediction noise as σ_p = 1, $\sigma_v = 0.5$, $\sigma_\alpha = 0.05$.

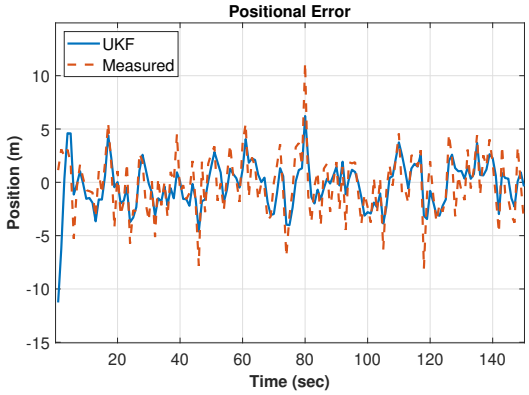

Fig. 16: Error in UKF

The above figure shows error in the prediction of position when the vehicles are moving in third order dynamics and using location sensor to measure the position. UKF performs effectively with better accuracy and less data rate as it does not require the sensor fusion for receiving velocity and acceleration values as seen from Table III. The maximum error in measurement for a third order dynamic movement can be see to be around 12 meters, whereas the predicted error pos_e is less than 5 meters.

VII. Beamforming

A. Beamforming and vehicle Alignment

The above Fig. 17 shows the effect of beam switching$\Delta\theta$ and beamforming angle ψ. The hardware designing for these two parameters has been elaborated in later section, however it is to be noted that the $\Delta\theta$ is due to the phase shifters in all beamforming - Analog, Digital and Hybrid beamforming. The beam shape is the result of the weighted or non-weighted inputs the Antenna elements. Thus as the phase shifters increase, the beam steering will have a higher sensitivity and higher number of elements will have narrow beams. Although they have different subsystems, the implementation needs to consider the effects for $\Delta\theta$ and ψ.

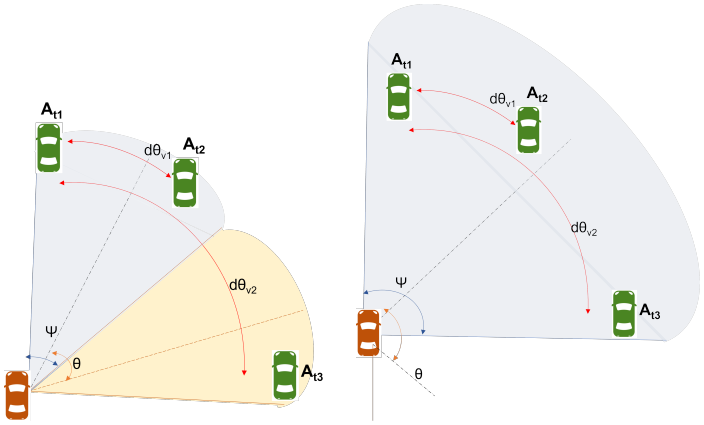

Fig. 17: Beam switching for different ψ

In the proposed work, the two vehicles are supposed to be in sustainable link L if they are in the beam coverage area. Although a beam switch, that is increment in θ by the sensitibity $\Delta\theta$ will have no effect on L if $\Delta\theta \leq \psi$. In the Fig. 17a, the $d\theta$ or $\Delta\theta$ is calculated based on their $pos_{A,t}$ at three different time instants. The proposed system does not initiate a beam switch, $(theta_{t1} = \theta_{t2}$ since the radial difference in angle is less than ψ. The unwanted shifts maintain the link stability, improve power consumption and reduce communication over head. Especially when both the vehicles are moving in parallel lanes, the contact time can be very less, making it critical to use the communication channel very efficiently. In the given scenario, the beam steering algorithm is assumed to have full efficiency and optimization. However, if an exhaustive search algorithm has to be implemented, every beam steer which might result in reiterating the beam steering algorithm with temporary loss of commmunication link.

At position $pos_{A,t3}$, the system in Fig. 17a, requires a shift wheres as the wider ψ in Fig. 17b can continue to reuse the same beam without any additional beam steer losses.

B. KF on beamwidth

The error in beam alignment can be compensated with beam width ψ so that the vehicle B remains in communication link. As seen for measured error can be ± 10 degrees with wider beams where as for Kalman filtered values, the less error can afford narrow beams.

In the Fig. 18 we can see the effect of dual mode localization observed in figure 8 on the beam alignment of vehicle B. This figure also establishes a relation between beamwidth ψ and beam alignment angle θ. The actual angle between the two vehicles is given be θ_{veh}. However for a certain beamwidth ψ, it is not required to adjust θ for every time instant. This constrain is given by the equation

$$\psi \leq \Delta\theta = \theta_{t+1} - \theta_t \tag{24}$$

As the vehicle B approaches the leader vehicle A (t_0 to $t_7 5$), θ_{veh} changes non-linearly since it is proportional to the tangent of the distance between them. Thus the value of $\Delta\theta$ is not constant for every time instant and increases during the event

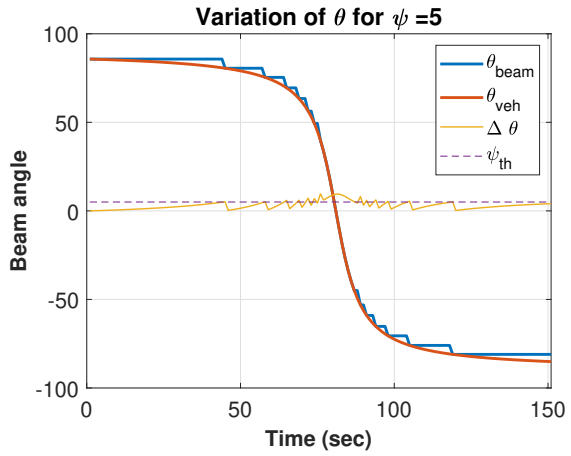

Fig. 18: Beam tracking for first order

of overtake. When $\Delta\theta$ increases above the ψ threshold, the vehicle communication link disrupts as vehicle A is outside the coverage area of vehicle B.

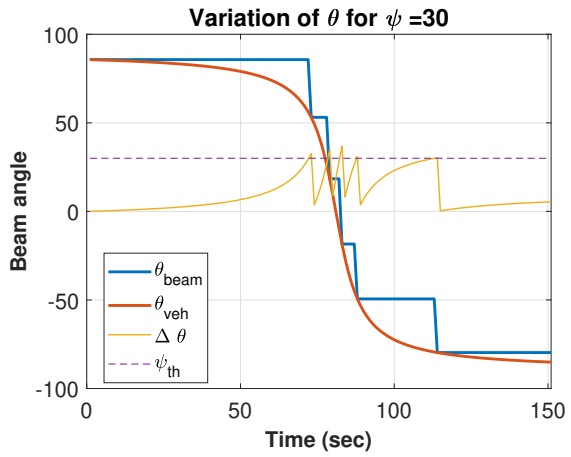

Fig. 19: Beam tracking

Smaller ψ increases the SNR but the system complexity increases as the beam switching instances (seen as steps in θ_{beam}). As seen in figure 19, as the ψ increases, the number of switching instances have been reduced to 5 from 25 in figure 18. The beam alignment complexity further increases with higher order vehicle dynamics and adaptive beamformings.

C. Classification of Beam forming

In passive architectures the beam can be steered not only to discrete but virtually any angle using active beamforming antennas. True to its name, this type of beamforming is achieved in the analog domain at RF frequencies or an intermediate frequency [33]. Digital beamforming supports higher RF chains and higher flexibility regarding the transmission and reception. The additional degree of freedom can be leveraged to perform advanced techniques like multi-beam MIMO [34] . Hybrid beamforming has been proposed as a possible solution that is able to combine the advantages of both analog and digital beamforming architectures [35].The cost reduction and power efficiency can be achieved by reducing the number of complete RF chains. This does also lead to lower overall power consumption. Since the number of converters is significantly lower than the number of antennas, there are less degrees of freedom for digital baseband processing.

D. Array Factor

As per [36], the angular resolution and the directivity of beamwidth is given as,

$$D = P_{max}/P_{avg} \tag{25}$$
$$G = kD \tag{26}$$
$$k = P_{rad}/P_{in} \tag{27}$$
$$D = 4\pi/\theta_1\theta_2 \tag{28}$$

where D is Directivity, G is Antenna Gain, k is Antenna Losses, For 3D, θ_1 and θ_2 are the azimuth and elevation angles.

For an array, Antenna gain= single element gain. Beamforming array gain

$$AF, \psi = \frac{sin(N[\frac{\pi d}{\lambda}sin\theta - \frac{\Delta\Phi}{2}])}{Nsin(\frac{\pi d}{\lambda}sin\theta - \frac{\Delta\Phi}{2})} \tag{29}$$

where N is number of elements.

E. Beamwidth Resolution

For ULAs, approximate HPBW By substituting 3 dB down in AF for HPBW,and equating it with $1/\sqrt{(2)}$. The effect of N on ψ is also simulated in the works of [37].

$$\psi = \frac{0.886\lambda}{Ndcos\theta} \tag{30}$$

Thus for $N = 16, \psi = 6°$ and $N = 32, \psi = 3°$.

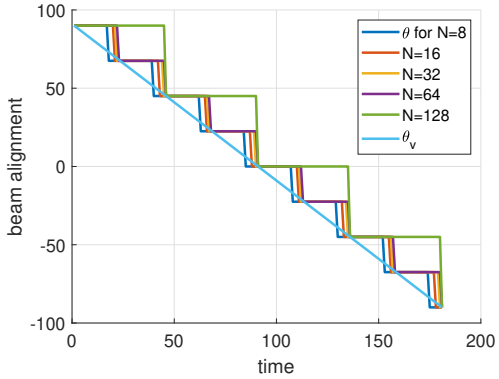

Fig. 20: Beamforming accuracy: Variation for N element antenna array

In the above Fig. 20, the Beam alignment is implemented using a 3 bit phase shifter for varying antenna elements. As seen, for higher array elements, the beam becomes more narrow and the ψ reduces as seen in Eq. 30

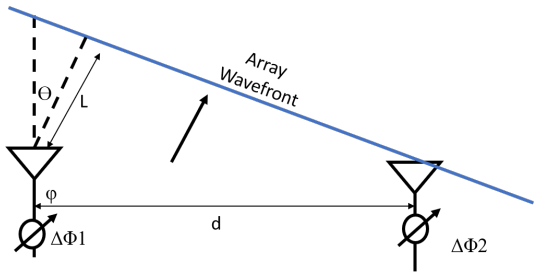

Fig. 21: Antenna Phased Array

VIII. Beam Steering

A. Design of Phased Array

The beam is pointed in a direction off boresight,θ, which is an angle, φ, from the horizon. Each element separated by a distance (d). The time delay to steer our beam is equal to the time it will take for the wavefront to traverse that distance, L. Based on the works of [38].

$$cos\varphi = L/d \tag{31}$$

$$L = dcos\Psi \tag{32}$$

$$= dsin\theta \tag{33}$$

$$\Delta\Phi = 2\pi dsin\theta/\lambda \tag{34}$$

$$\Delta\Phi = \pi sin\theta \tag{35}$$

Thus for θ of 30 ° , the phase shift $\Delta\Phi$ is 90 °. So, if our wavefront is arriving at θ = 30°, and we then shift the phase of the neighboring element by 95°, we will cause the individual signals of both elements to add coherently. This will maximize the antenna gain in that direction. The hardware implementation of such phase shifters has been explained in [39] [40]

B. Beam steering Resolution

As per [41], Using digital microwave phase shifters calculated phase shift must be approximated according to phase shifter resolution, then accuracy of beam positioning is equal few degrees. Application of optical weigh units in phase array beam forming provide fully antenna characteristic control. Very high resolution and an excellent accuracy of the antenna beam positioning can be achieved. Optimal technique depends on number of antenna elements, which implicates beam width.

Thus the equation for beam steer is [42],

$$\Delta\theta = \frac{360\circ}{2^n} \tag{36}$$

where n is the number of bits in digital phase shifter and its accurate calibration methodology is explained in [42]

In the Fig. 22, the effect Hardware designing on implementing the beam alignment is studied. As seen in Eq. , as the number of bits in phase shifters increase, the $\delta\theta$ reduces which increases the beam alignment accuracy. The goal of the system is to align the beam angle θ with the vehicle angle θ_v. For 1 bit, the Antenna system can have only 2 values, $\pm$90, whereas

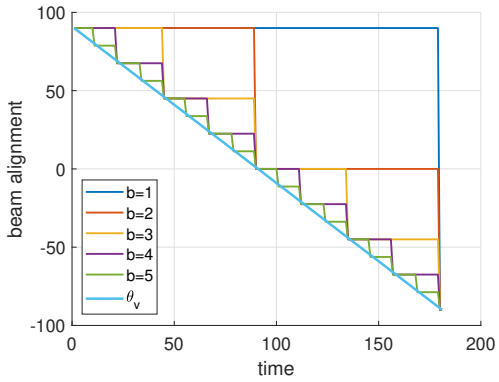

Fig. 22: Beam alignment error

for For a 5 bit phase shifter, resolution $\theta = 360/32 = 11.25°$ with an error of 5.625 ∘.

IX. Channel Quality of Service

A. Variation with positional error

The following graphs have been plotted for positional error in distance $d_e = 2m$ and $d_e = .1m$ for vehicle A from time t=0 to 300 secs. The effective error in beam alignment angle is θ_e.

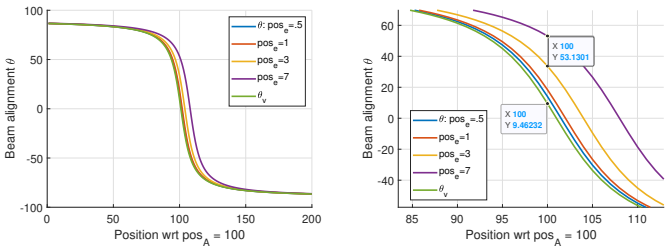

Fig. 23: Effect of positional error on θ

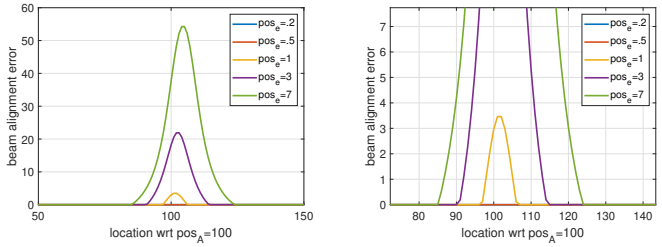

Fig. 24: Beam alignment error θ_e

For single mode communication with $va = 0$, $vb = 5$,$R = 80$. It is similar to figure 19. The values of error are derived from figure 14 .

$$\theta_e = \tan^{-1}\frac{|pos_a - pos_b| + d_e}{w} - tan^{-1}\frac{|pos_a - pos_b| - d_e}{w} \tag{37}$$

Similar to Eq(4), where w is width of road = 6m.

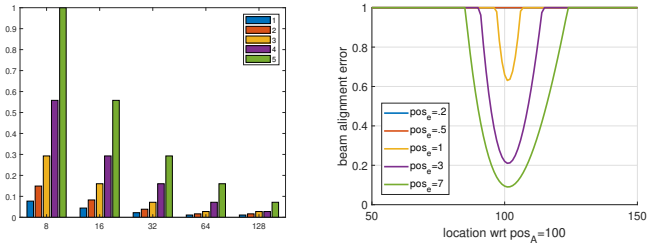

Fig. 25: Link Accuracy for various phase shifters and Antenna elements

The above Fig. 25, explains the effect of phase shifter in the sensitivity of θ and number of elements on the Beamforming angle ψ. The increase in phase shifters for Digital or Hybrid beamforming increases the RF chains used in the Antenna System, however it is common to see a 5 bit phase shifter. In fig. 25b, the effect of positional error for a beam alignment scenario is explained. In this event the receiver vehicle A is present at position 100 and the transmitter ego vehicles passes it over a range of 200 meters, from 0 to 200. The error increases especially when the relative distance between them is less than 20 meters for a road width of 6 meters based on Eq. 4. The probability of a successful link can be given as

$$L = 1, \text{If } l_\psi \geq pos_e \tag{38}$$

$$Pr_{L=1} = \frac{pos_e - l_\psi}{pos_e} \tag{39}$$

$$l_\psi = w[tan(\theta_v + \psi/2) - tan(\theta_v)] \tag{40}$$

The probability of link is calculated based on the ratio of estimated length covered by transmitter beam(l_ψ) to the Positional Error length (pos_e) predicted using UKF. As seen in Fig. 25b, the positional error pos_e can be seen as a function of pos and thus the θ_v.

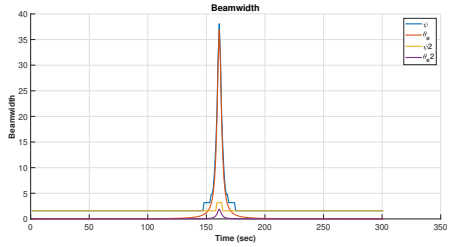

Fig. 26: Beamwidth ψ

The figure shows expected ψ and ψ_{actual}. This is due to hardware constraints based on phase shifters explained in beam steer resolution. Thus the actual beamwidth will always be in the multiple of $\Delta\psi$ as seen in above figure.

$$FSPL = (\frac{4\pi df}{c})^2 \tag{41}$$

$$P_{sig}dB = P_{tx} + G_{tx} + G_{rx} - FSPL_{db} \tag{42}$$

$$P_n dB = Thermalnoise - NF \tag{43}$$

$$SNRdB = P_{sig} - P_n \tag{44}$$

In our previous work [43], the SNR was calculated for a dynamic environment, however in proposed work, the gain is function of position and the antenna directivity. This dependency is also explained in [44]. Using the Eq.44 for 28 GHz, with transmit power of 5 dB and an omnidirectional receiving antenna with unit gain, the SNR can plotted over a range of 100 meters. The thermal noise = kTB, where k is Boltzaman constant, at 294 K, and Bandwidth is 10% of the frequency. The noise factor is assumed to be 15dB.

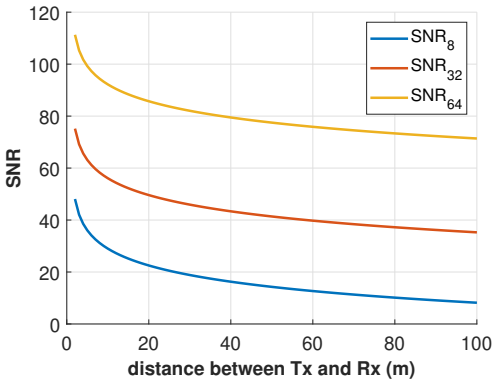

Fig. 27: SNR

Based in Fig .27 and Eq. 44, it can be seen that SNR is high when the transmitter receiver distance is low. As the number of elements in the antenna increase from 8, 32 to 64, the beam becomes more directional as seen in Eq. 30. This increase in directivity improves the Antenna transmit gain G_tx. In our previous work, [43] [45], the effect of SNR on dynamic system has been elaborated for the above equations. In this work, the gain of the system is function of Antenna elements for directional phassed array structure. This effect of narrow beams has been shown in terms of improvement in the SNR.

The future goal would be to optimize the overall system based on the Fig. 25 and Fig. 27 to design a highly sustainable link in vehicle dynamic system.

The probability of connection link Pr_L for the dynamic V2V L, was shown in Fig.25b and Eq. 40. For number of elements N=64 and the positional errors of 0, 0.5,1 3 and 7 meters , the link drops especially during the event of overtake. The reason is the beam coverage area for close distance is low thus reducing the communication link probability. Although the narrower beam increases the SNR, this problem is much severe here. This is illustrated in the above Fig. 28 where we can see, for a the positional error of 7m, the SNR reduces more than 90 % of its value.

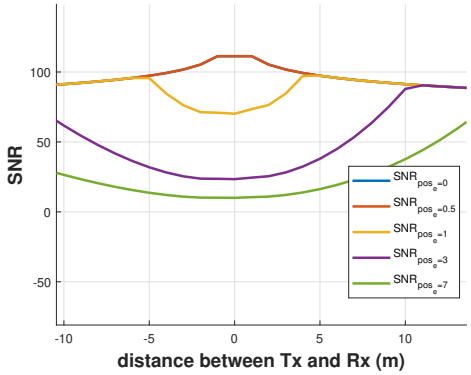

Fig. 28: Effect of positional error on SNR

X. Conclusion

An interdisciplinary approach to the V2V communication using Vehicle Dynamics, Beamforming and Beam steering is proposed, and the simulation models elaborate the high dimensional interplay among them. This study aims to simulate conditions such as higher-order dynamics and constraints at antenna hardware-level implementation to reduce the gap in theoretical and real-time conditions. The work includes system models such as Prediction and Antenna Phased array whose performance affects the link quality and sustainability while considering a V2V scenario and dual-mode localization. The above work has designed a model for third-order vehicle dynamics using non-linear acceleration. The sensor noise introduced due to GPS positional awareness and communication delay was reduced using Unscented Kalman Filter. The optimization of Beam alignment and narrow beamwidth led to increased directivity and improved SNR. However, the effect of such directional beams on the link quality for a localizing vehicle was analyzed. The paper presents extensive Matlab simulations to address the existing research gap for dual-mode localization in V2V communication along with the theoretical proofs. The paper attempts to strengthen the joint approach of vehicle dynamics and V2V communication using the Kalman filter to improve its practicability.

XI. Acknowledgement

The research is supported by the NSF (award# 2010366 and #2140729).

References

[1] H. Kang, S. Montejo-Sánchez, C. A. Azurdia-Meza, and S. Céspedes, "Beamforming for Beaconing in V2V Communications," in *2019 IEEE XXVI International Conference on Electronics, Electrical Engineering and Computing (INTERCON)*, Aug. 2019, pp. 1–4.

[2] Y. A. Harfouch, S. Yuan, and S. Baldi, "An Adaptive Switched Control Approach to Heterogeneous Platooning With Intervehicle Communication Losses," *IEEE Transactions on Control of Network Systems*, vol. 5, no. 3, pp. 1434–1444, Sep. 2018, conference Name: IEEE Transactions on Control of Network Systems.

[3] B.-J. Chang, R.-H. Hwang, Y.-L. Tsai, B.-H. Yu, and Y.-H. Liang, "Cooperative Adaptive Driving for Platooning Autonomous Self Driving Based on Edge Computing," *International Journal of Applied Mathematics and Computer Science*, vol. 29, no. 2, pp. 213–225, Jun. 2019. [Online]. Available: https://www.sciendo.com/article/10.2478/amcs-2019-0016

[4] F. N. Alsaleem, J. S. Thompson, and D. I. Laurenson, "Adaptive Sum of Markov Chains for Modelling 3D Blockage in mmWave V2I Communications," *IEEE Transactions on Vehicular Technology*, vol. 69, no. 9, pp. 9431–9444, Sep. 2020, conference Name: IEEE Transactions on Vehicular Technology.

[5] C. Ballesteros, G. Ramírez, L. Montero, J. Romeu, and L. Jofre, "Study on Beamforming V2I Scenarios for Sub-6 GHz and mmWave Channels," in *2020 14th European Conference on Antennas and Propagation (EuCAP)*, Mar. 2020, pp. 1–5.

[6] C. Mahabal, H. Fang, and H. Wang, "Adaptive vehicle platooning using joint network traffic approach," in *GLOBECOM 2021 - 2021 IEEE Global Communications Conference*, 2021.

[7] Y. M. Tsang, A. S. Y. Poon, and S. Addepalli, "Coding the Beams: Improving Beamforming Training in mmWave Communication System," in *2011 IEEE Global Telecommunications Conference - GLOBECOM 2011*, Dec. 2011, pp. 1–6, iSSN: 1930-529X.

[8] N. Kanthasamy, R. Du, K. S. Gill, A. M. Wyglinski, and R. Cowlagi, "Assessment of Positioning Errors on V2V Networks Employing Dual Beamforming," in *2018 IEEE 88th Vehicular Technology Conference (VTC-Fall)*, Aug. 2018, pp. 1–5, iSSN: 2577-2465.

[9] X. Chen, X. Liu, Z. Zhu, and K. Ao, "Strategy research on vehicle constant speed downhill control based on hydraulic retarder," in *2017 2nd Asia-Pacific Conference on Intelligent Robot Systems (ACIRS)*, Jun. 2017, pp. 156–159.

[10] A. Rakhshan and H. Pishro-Nik, "Packet success probability derivation in a vehicular ad hoc network for a highway scenario," in *2016 Annual Conference on Information Science and Systems (CISS)*. Princeton, NJ, USA: IEEE, Mar. 2016, pp. 210–215. [Online]. Available: http://ieeexplore.ieee.org/document/7460503/

[11] G. Fiengo, D. G. Lui, A. Petrillo, S. Santini, and M. Tufo, "Distributed Robust PID Control For Leader Tracking in Uncertain Connected Ground Vehicles With V2V Communication Delay," *IEEE/ASME Transactions on Mechatronics*, vol. 24, no. 3, pp. 1153–1165, Jun. 2019, conference Name: IEEE/ASME Transactions on Mechatronics.

[12] F. Liu and C. Masouross, "A tutorial on joint radar and communication transmission for vehicular networks—part iii: Predictive beamforming without state models," *IEEE Communications Letters*, vol. 25, no. 7, 2021.

[13] Y.-Y. Lin and I. Rubin, "Infrastructure aided networking and traffic management for autonomous transportation," in *2017 Information Theory and Applications Workshop (ITA)*, Feb. 2017, pp. 1–7.

[14] M. Yamakado and M. Abe, "Proposal of the longitudinal driver model in coordination with vehicle lateral motion based upon jerk information," in *2008 International Conference on Control, Automation and Systems*, Oct. 2008, pp. 2896–2901.

[15] Y. S. Kim, J. Park, T. W. Park, J. S. Bang, and H. S. Sim, "Anti-jerk controller design with a cooperative control strategy in Hybrid Electric Vehicle," in *8th International Conference on Power Electronics - ECCE Asia*, May 2011, pp. 1964–1968, iSSN: 2150-6086.

[16] J. Wu and P. Fan, "A Survey on High Mobility Wireless Communications: Challenges, Opportunities and Solutions," *IEEE Access*, vol. 4, pp. 450–476, 2016, conference Name: IEEE Access.

[17] X. Zhang, S. Pan, and Q. Miao, "Adaptive Beamforming-Based Gigabit Message Dissemination for Highway VANETs," *IEEE Transactions on Intelligent Transportation Systems*, pp. 1–14, 2021, conference Name: IEEE Transactions on Intelligent Transportation Systems.

[18] *Global Positioning System (GPS) Standard Positioning Service (SPS) Performance Analysis Report*, GPS Product Team,Washington, DC, USA, 2014.

[19] A. Deep, M. Mittal, and V. Mittal, "Application of Kalman Filter in GPS Position Estimation," in *2018 IEEE 8th Power India International Conference (PIICON)*, Dec. 2018, pp. 1–5, iSSN: 2642-5289.

[20] X. Shen, Y. Liao, X. Dai, M. Zhao, K. Liu, and D. Wang, "Joint channel estimation and decoding design for 5G-enabled V2V channel," *China Communications*, vol. 15, no. 7, pp. 39–46, Jul. 2018, conference Name: China Communications.

[21] S. G. Larew and D. J. Love, "Adaptive Beam Tracking with the Unscented Kalman Filter for Millimeter Wave Communication,"

arXiv:1804.08640 [cs, eess, math], Apr. 2018, arXiv: 1804.08640. [Online]. Available: http://arxiv.org/abs/1804.08640

[22] A. H. Sakr, G. Bansal, V. Vladimerou, K. Kusano, and M. Johnson, "V2V and on-board sensor fusion for road geometry estimation," in *2017 IEEE 20th International Conference on Intelligent Transportation Systems (ITSC)*, Oct. 2017, pp. 1–8, iSSN: 2153-0017.

[23] O. Karoui, M. Khalgui, A. Koubâa, E. Guerfala, Z. Li, and E. Tovar, "Dual mode for vehicular platoon safety: Simulation and formal verification," *Information Sciences*, vol. 402, pp. 216–232, Sep. 2017. [Online]. Available: http://www.sciencedirect.com/science/article/pii/S0020025517305959

[24] P. Nilsson, L. Laine, N. van Duijkeren, and B. Jacobson, "Automated highway lane changes of long vehicle combinations: A specific comparison between driver model based control and non-linear model predictive control," in *2015 International Symposium on Innovations in Intelligent SysTems and Applications (INISTA)*, 2015, pp. 1–8.

[25] S. S. K. Puranam, A. Gopinath, and R. Sainati, "Amplitude based beam steering," in *2019 IEEE International Symposium on Phased Array System Technology (PAST)*, 2019, pp. 1–4.

[26] W. C. Chen, "5G mmWAVE Technology Design Challenges and Development Trends," in *2020 International Symposium on VLSI Design, Automation and Test (VLSI-DAT)*, Aug. 2020, pp. 1–4, iSSN: 2472-9124.

[27] D. Simon, "Kalman filtering," in *Embed. Syst. Program*, 2001, pp. 72–79.

[28] Q. Li, R. Li, K. Ji, and W. Dai, "Kalman filter and its application," in *2015 8th International Conference on Intelligent Networks and Intelligent Systems (ICINIS)*, 2015, pp. 74–77.

[29] A. Deep, M. Mittal, and V. Mittal, "Application of kalman filter in gps position estimation," in *2018 IEEE 8th Power India International Conference (PIICON)*, 2018, pp. 1–5.

[30] E. Wan and R. Van Der Merwe, "The unscented Kalman filter for nonlinear estimation," in *Proceedings of the IEEE 2000 Adaptive Systems for Signal Processing, Communications, and Control Symposium (Cat. No.00EX373)*. Lake Louise, Alta., Canada: IEEE, 2000, pp. 153–158. [Online]. Available: http://ieeexplore.ieee.org/document/882463/

[31] X. Shen, Y. Liao, and X. Dai, "BEM-based UKF Channel Estimation for 5G-enabled V2V Channel," in *2018 IEEE Global Conference on Signal and Information Processing (GlobalSIP)*, Nov. 2018, pp. 1214–1217.

[32] P. Pasek and P. Kaniewski, "Unscented Kalman filter application in personal navigation," in *Radioelectronic Systems Conference 2019*, vol. 11442. International Society for Optics and Photonics, Feb. 2020, p. 114421C. [Online]. Available: https://www.spiedigitallibrary.org/conference-proceedings-of-spie/11442/114421C/Unscented-Kalman-filter-application-in-personal-navigation/10.1117/12.2564984.short

[33] P. Kasemir, N. Sutton, M. Radway, B. Jeong, T. Brown, and D. S. Filipovič, "Wideband analog and digital beamforming," in *2009 9th International Conference on Telecommunication in Modern Satellite, Cable, and Broadcasting Services*, 2009, pp. 372–375.

[34] "Millimeter-Wave Beamforming: Antenna Array Design Choices & Characterization," p. 28.

[35] S. Jain, A. Markan, and C. Markan, "Performance evaluation of a millimeter wave mimo hybrid beamforming system," in *2020 IEEE Latin-American Conference on Communications (LATINCOM)*, 2020, pp. 1–5.

[36] A. Lagunas, O. Domínguez, and C. del Río, "A critical review of angular resolution vs. beamwidth in antenna systems," in *2017 IEEE MTT-S International Conference on Numerical Electromagnetic and Multiphysics Modeling and Optimization for RF, Microwave, and Terahertz Applications (NEMO)*, 2017, pp. 134–136.

[37] D. N. Patel, B. J. Makwana, and P. B. Parmar, "Comparative analysis of adaptive beamforming algorithm lms, smi and rls for ula smart antenna," in *2016 International Conference on Communication and Signal Processing (ICCSP)*, 2016, pp. 1029–1033.

[38] N. Nakamoto, T. Takahashi, Y. Konishi, and I. Chiba, "Phase optimization for accurate beam forming of phased array with element field errors at every phase shift," in *2013 IEEE International Symposium on Phased Array Systems and Technology*, 2013, pp. 693–697.

[39] S. I. M. Sheikh, A. A. P. Gibson, M. Basorrah, G. Alhulwah, K. Alanizi, M. Alfarsi, and J. Zafar, "Analog/Digital Ferrite Phase Shifter for Phased Array Antennas," *IEEE Antennas and Wireless Propagation Letters*, vol. 9, pp. 319–321, 2010, conference Name: IEEE Antennas and Wireless Propagation Letters.

[40] M. Nikfalazar, M. Sazegar, A. Mehmood, A. Wiens, A. Friederich, H. Maune, J. R. Binder, and R. Jakoby, "Two-Dimensional Beam-Steering Phased-Array Antenna With Compact Tunable Phase Shifter Based on BST Thick Films," *IEEE Antennas and Wireless Propagation Letters*, vol. 16, pp. 585–588, 2017, conference Name: IEEE Antennas and Wireless Propagation Letters.

[41] M. Muszkowski and E. Sedek, "Accuracy Analysis of Phase Array Antennas Beam Steering Based on Digital Phase Shifters and Fibre Optic Delay Lines."

[42] K. Temir, M. S. Akyüz, and Y. K. Alp, "Consideration of environmental and functional factors in calibration of antenna integrated active phased array transmitters," in *2016 IEEE International Symposium on Phased Array Systems and Technology (PAST)*, Oct. 2016, pp. 1–5.

[43] C. Mahabal, H. Fang, and H. Wang, "Smart spectrum switching and beamforming for wireless body area networks in dynamic environment," *Journal of Communications and Information Networks*, vol. 5, no. 2, pp. 204–216, 2020.

[44] E. A. Firouzjaei, "mm-Wave Phase Shifters and Switches," p. 114.

[45] C. Mahabal, H. Fang, and H. Wang, "Smart spectrum switching in wireless body area networks," in *GLOBECOM 2020 - 2020 IEEE Global Communications Conference*, 2020, pp. 1–6.